

# Delocalization of Charge and Electron Density in the Humulyl Cation—Implications for Terpene Biosynthesis

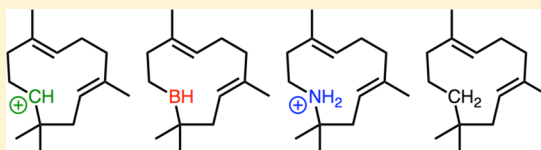
Trevor A. Hamlin,<sup>‡,†</sup> Christian S. Hamann,<sup>\*,‡</sup> and Dean J. Tantillo<sup>\*,§</sup>

<sup>‡</sup>Department of Chemistry and Biochemistry, Albright College, 13th and Bern Streets, Reading, Pennsylvania 19604, United States

<sup>§</sup>Department of Chemistry, University of California—Davis, 1 Shields Avenue, Davis, California 95616, United States

**S** Supporting Information

**ABSTRACT:** The stabilizing features of a macrocyclic sesquiterpene-derived cation were explored using quantum mechanical calculations. The monocyclic humulyl cation, the product of 11,1-cyclization of farnesyl diphosphate, is the product of the first committed step in the enzymatic synthesis of a range of structurally diverse sesquiterpenes, including humulene (monocyclic); caryophyllene (bicyclic); and protoilludene, pentalene, and isocomene (tricyclic). These natural products are formed via carbocation cascades that are directed in part by the conformation of the humulyl cation. Understanding the mechanistic details of product formation requires an understanding of the conformational preferences of this fundamental intermediate. Replacing the carbocation with borane (preserving  $\pi$ -accepting capabilities), ammonium (preserving positive charge), and methylene (preserving neither  $\pi$ -accepting capabilities nor charge) provides a systematic method to distinguish electrostatic and orbital effects on structure and internal stabilization. Several modes of internal stabilization—hyperconjugation, transannular  $\pi(\text{alkene})\cdots\text{C}^+$  and transannular  $\text{C}-\text{H}\cdots\text{C}^+$  interactions—were uncovered, confirming and extending previous studies on this and similar systems.



## INTRODUCTION

The humulyl cation (1) is a proposed intermediate generated in the active sites of various sesquiterpene synthases en route to a diverse group of mono- and polycyclic sesquiterpene natural products containing 11-membered rings (representative examples are shown in Scheme 1).<sup>1</sup> Unlike most secondary carbocations proposed as intermediates in terpene-forming carbocation cascades, the humulyl cation appears to be a true

minimum on the  $\text{C}_{15}\text{H}_{25}^+$  potential energy surface.<sup>2,3</sup> By analyzing the conformations of the humulyl cation, we can begin to understand the stereoelectronic requirements of various pathways leading to an expansive product distribution. The stabilizing factors (hyperconjugation, transannular  $\pi(\text{alkene})\cdots\text{C}^+$  and transannular  $\text{C}-\text{H}\cdots\text{C}^+$  interactions) that allow secondary carbocations to be minima were uncovered with the aid of density functional theory calculations.<sup>3</sup> The effects of charge and hybridization at the carbocation center in the humulyl cation were assessed via comparisons with  $\text{CH}^+ \rightarrow \text{BH}$  (preserves hybridization, but not charge),  $\text{NH}_2^+$  (preserves charge, but not hybridization) and  $\text{CH}_2$  (preserves neither hybridization nor charge) congeners (2–4, Chart 1, Table 1) of various humulyl cation conformers (the complete, complex

Scheme 1

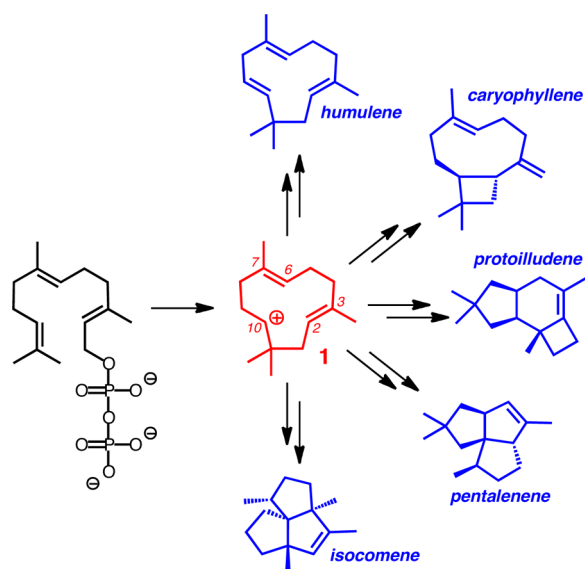
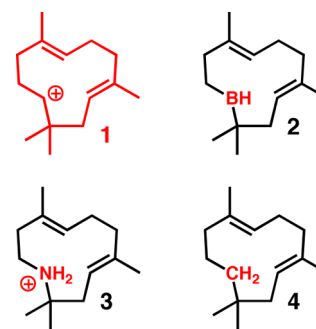


Chart 1



Received: February 17, 2015

Published: March 30, 2015

**Table 1. Systematic Substitution of the Carbenium Ion at Position 10 in the Humulyl Cation**

position 10	probe	empty p-orbital	formal charge
R <sub>2</sub> CH	(starting material)	yes	+1
R <sub>2</sub> BH	borane substitution	yes	0
R <sub>2</sub> NH <sub>2</sub>	ammonium substitution	no	+1
R <sub>2</sub> CH <sub>2</sub>	methylene substitution	no	0

conformational potential energy surface for the humulyl cation will be described in a separate report).<sup>4</sup> By characterizing the features that internally stabilize various conformers of the humulyl cation, we reveal which structural features a sesquiterpene-synthesizing enzyme would have to avoid disrupting, enhance or overcome to bind to (externally stabilize) a specific conformer.<sup>4</sup>

## METHODS AND DATA PRESENTATION

All calculations were performed with Gaussian03 or Gaussian 09.<sup>5</sup> Geometries were optimized using the B3LYP/6-31+G(d,p) method.<sup>6</sup> The B3LYP method has been used previously to characterize energy surfaces for carbocation rearrangements.<sup>3a</sup> Despite shortcomings in treating dispersion,<sup>7</sup> specifically in capturing relative energies of cyclic versus acyclic isomers,<sup>3</sup> we feel that this method is appropriate for the questions addressed herein, which primarily involve isomers with a single (macrocyclic) ring. For tests on the structure shown in Figure 1d using other methods (M06, MP2), see the Supporting Information. Stationary points were characterized by frequency calculations at 298 K, with structures at energy minima showing no imaginary frequencies and transition state structures showing one imaginary frequency. Intrinsic reaction coordinate (IRC) experiments<sup>9</sup> were run to assess the effect of atomic substitutions on molecular geometry and bonding during transit between associated minima through a common transition state structure (see Supporting Information). Electronic energies are reported in kcal mol<sup>-1</sup>; bond lengths are reported in angstroms (Å); bond and dihedral angles are presented in degrees (deg). Pyramidalization was measured as the sum of the bond angles around particular atomic centers and ranges from 360° (trigonal

planar) to 328.5° (trigonal pyramidal in the extreme case of tetrahedral bond angles).

Starting structures were derived from our ongoing investigations into the conformations of the humulyl cation, which contains a carbenium ion center at C<sub>10</sub> (atom numbering is shown in Scheme 1). Using several minima and transition-state structures, we systematically substituted carbenium ion centers as shown in Chart 1. Each structure was subjected to geometry optimization and frequency analysis. Structural drawings were produced using *Ball & Stick*.<sup>10</sup>

Imaginary frequencies whose corresponding molecular motion involved either the substituent at the X<sub>10</sub> position wagging into and out of the center of the cyclic molecule (tending to explore hyperconjugation, transannular cation- $\pi$  interactions,<sup>11</sup> and/or carbon-carbon bond formation) or the C<sub>6</sub>-C<sub>7</sub> prenyl flip that orients the vinyl C<sub>6</sub>-H toward the substituent at the X<sub>10</sub> position (tending to explore transannular C-H- $\pi$  interactions<sup>12</sup>) were targeted in this study. Analysis of the C<sub>2</sub>-C<sub>3</sub> prenyl flip in these structures served as a control for these experiments (see Supporting Information).

Atomic substitution is a time-honored investigative tool but is not without its shortcomings. Periodic trends in atomic size and electronegativity plus variability in the subtle details of structure between subvalent and fully valent atoms have the potential to derail atomic substitution studies. We explicitly address these inherent limitations with thorough IRC analysis of stationary points (both in the text and in the Supporting Information). The IRC results indicate that the humulyl framework is structurally flexible enough to accommodate the small changes in C-X bond length such that artifacts arising from that parameter do not change the overall comparison to the parent carbenium ion. In addition, the IRCs allow the electrostatic and orbital interactions to be explored during conformational transitions, an appropriate and thorough probe of potential interactions or lack thereof.

For all schematics of computed structures, typical atom coloring is used (carbons in black, hydrogens in white, nitrogens in blue) with the following modifications: carbocation centers are colored green, carbons in C=C  $\pi$ -bonds are colored red; boron atoms are colored pink, intramolecular contacts involving  $\pi$ -bonds or C<sub>sp<sup>2</sup></sub>-H bonds are indicated with red dotted lines, distances associated with C=C bonds are shown in red, and lengths of strongly hyperconjugated<sup>13</sup> C-C bonds ( $\geq 1.60$  Å) are shown in green.

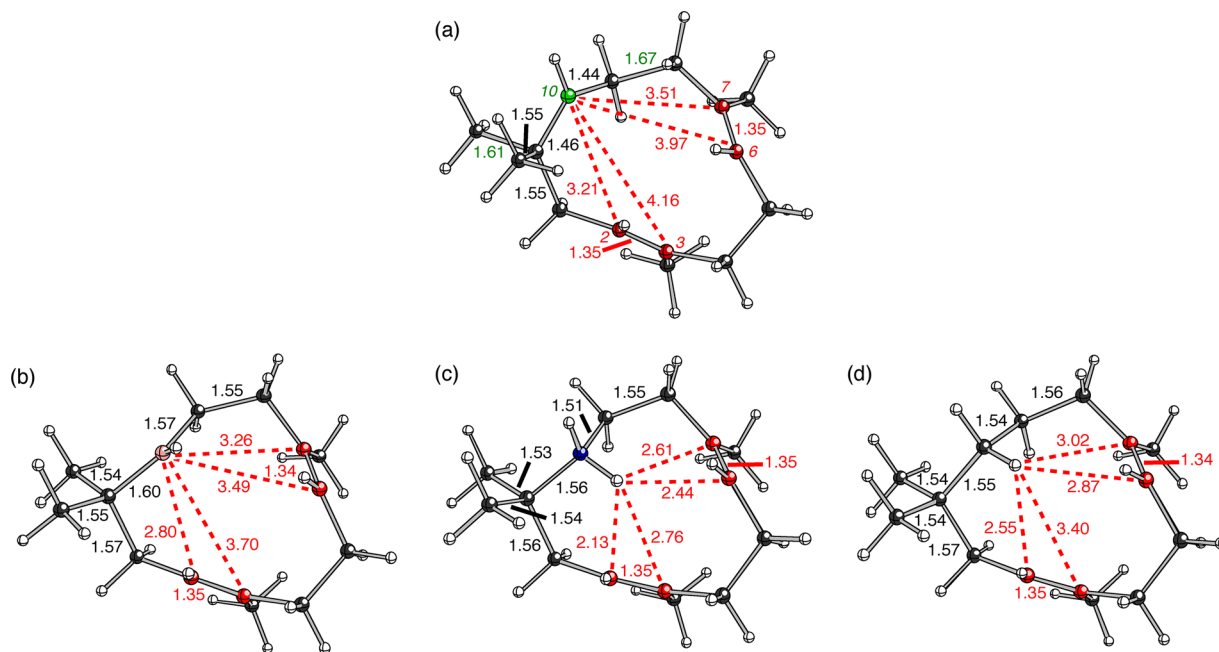


**Figure 1.** (a) Representative conformer of the humulyl cation with C-C bonds elongated due to hyperconjugation (green), along with (b) CH<sup>+</sup> → BH, (c) CH<sup>+</sup> → NH<sub>2</sub><sup>+</sup>, and (d) CH<sup>+</sup> → CH<sub>2</sub> congeners. Selected distances are shown in Å.

## RESULTS AND DISCUSSION

**1. Hyperconjugation.** Many conformers of the humulyl cation are stabilized by hyperconjugation,<sup>13</sup> characterized by elongated C–C bond lengths, typically on the order of 1.6–1.7 Å. In many cases, more than one C–C bond is lengthened relative to a “nominal” 1.53–1.55 Å C<sub>sp3</sub>–C<sub>sp3</sub> bond. A representative conformer is shown in Figure 1a. Note that two C–C bonds are elongated to >1.6 Å. Although the CH<sup>+</sup> → BH congener still contains a formally empty *p*-orbital, elongation of neighboring C–C bonds is not observed. C–C bond elongation is also not observed for the C<sup>+</sup> → NH<sub>2</sub><sup>+</sup> and CH<sub>2</sub> congeners, for which the electron-accepting *p*-orbital is not available. Thus, both a formally vacant *p*-orbital and a positive charge are necessary for strong hyperconjugation to occur, a result consistent with studies in other carbocationic systems.<sup>13</sup> Note also that variations in electronegativity also play a (presumably small) role; for example, C is more electronegative than B and N–H hydrogens bear more partial positive charge than C–H hydrogens.

**2. Transannular X–H⋯π(alkene) and π(alkene)⋯C<sup>+</sup> interactions.** For CH<sup>+</sup> → NH<sub>2</sub><sup>+</sup> congeners, transannular N–H⋯π interactions were often observed.<sup>1a,16</sup> For example, the ammonium ion shown in Figure 1c displays short contacts between one ammonium hydrogen and both C=C π-bonds. Removal of the positive charge, as for the hydrocarbon congener shown in Figure 1d, leads to a lengthening of these contacts. Transannular C–H⋯π interactions involving hyperconjugated C–H bonds have been observed for other macrocyclic carbocations,<sup>2a,12a</sup> but this type of interaction was not observed in any of the humulyl cation conformers located in our study. The humulyl cation appears more comfortable accommodating interactions between its π-bonds and the carbocation center itself. Further analysis of this phenomenon is presented below (see section 4).

Several humulyl cations that appear to be stabilized by transannular interactions between π-electron density in C=C π-bonds and the formally empty *p*-orbital at the carbocation center were located. Previous work established the ability of the transannular π(alkene)⋯C<sup>+</sup> interaction to influence the molecular rearrangements associated with terpene biosynthesis.<sup>2,3,12a</sup> A representative example from the humulyl system is shown in Figure 2a. While the carbocationic center in this structure is again engaged in hyperconjugation, it is not as dramatic as for the structure shown in Figure 1a. In the structure shown in Figure 2a, the carbocationic carbon is very slightly pyramidalized (sum of the three C–C–C/H angles at this center = 357°), the formally empty *p*-orbital at this center is directed toward the C<sub>6</sub>=C<sub>7</sub> π-bond, with C<sub>10</sub>⋯C<sub>6</sub> and C<sub>10</sub>⋯C<sub>7</sub> distances of 2.85 and 2.51 Å, respectively (distances to the C<sub>2</sub>=C<sub>3</sub> π-bond are greater: 3.05 and 3.78 Å), and the C<sub>6</sub>=C<sub>7</sub> π-bond is elongated slightly, to 1.37 Å. Such interactions have been observed in other carbocations,<sup>11,12</sup> in some cases with much shorter C<sup>+</sup>⋯π-bond distances (some short enough for the carbocations to be considered nonclassical).<sup>2,14</sup>

Although the borane congener of the conformer shown in Figure 2a displays the same overall geometric features (as evaluated by similarity between dihedral angles around the ring), the difference between the two structures is immediately evident (Figure 2b; note the longer B⋯C and shorter C=C distances). While B, like C<sup>+</sup>, has π-accepting capacity, the difference in their respective geometries is consistent with the cation–π interactions being largely electrostatic in nature. A

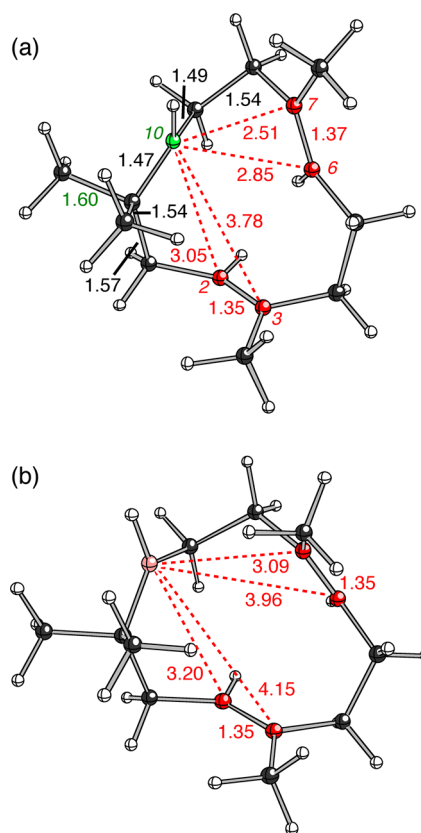


**Figure 2.** (a) Representative conformer of the humulyl cation displaying a transannular cation–π interaction and the (b) CH<sup>+</sup> → BH congener. Selected distances are shown in Å.

recent report proposes B⋯π-bond interactions with B⋯C distances as short as 3.3 Å,<sup>15</sup> but we see no evidence of such interactions, as the C<sub>2</sub>=C<sub>3</sub> double bond is of nominal length, nearly identical in length to the C<sub>6</sub>=C<sub>7</sub> bond length in this structure and the C=C bonds in other structures. In addition, the boron center is fully trigonal planar (sum of the three C–B–C/H angles at this center = 360°).

**3. Transannular C–H⋯C<sup>+</sup> Interactions.** The most unusual sort of stabilizing interactions found for the humulyl cation involves donation of electron density from C<sub>sp2</sub>–H bonds to the formally empty *p*-orbital at the carbocation center. A representative conformer that benefits from such an interaction is shown in Figure 3a. This structure shows significant pyramidalization at the carbocation center (sum of bond angles of 353°, as well as C<sub>sp2</sub>–H bond elongation (1.20 Å vs 1.09 Å for the “non-interacting” C<sub>sp2</sub>–H bonds in the same cationic structure). In addition, the C<sub>5</sub>–C<sub>6</sub>–C<sub>7</sub> bond angle increases from 127°–131° in all other structures examined up to 133°, and the C<sub>6</sub>=C<sub>7</sub> bond shortens to 1.33 Å, consistent with alkenyl cation character at C<sub>6</sub>.<sup>17</sup> Taken together, these data suggest that there is significant 3-center 2-electron bonding in this structure. 3-Center [C⋯H⋯C]<sup>+</sup> bonding arrays have been described previously for carbocations,<sup>18</sup> even ones related to terpene biosynthesis,<sup>19</sup> but, to our knowledge, these have not involved alkenyl carbons that tend toward sp-hybridization upon interaction (see Supporting Information). The borane congener shown in Figure 3b, a transition state structure for moving the alkenyl C–H group through the ring (C<sub>6</sub>,C<sub>7</sub>-prenyl flip), lacks 3-center 2-electron interactions, again highlighting the drive to delocalize charge, not just electron density, to

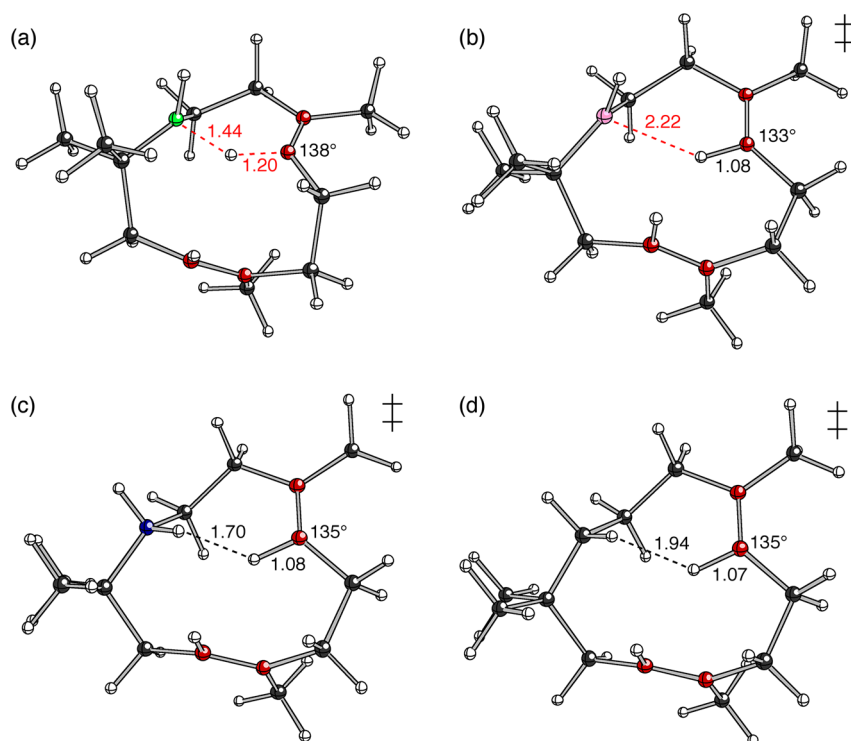


**Figure 3.** (a) A representative humulyl cation displaying the 3-center  $[C\cdots H\cdots C]^+$  interaction and (b-d)  $CH^+ \rightarrow BH$ ,  $NH_2^+$ , and  $CH_2$  congeners, respectively (all transition state structures for moving the  $C_{sp^2}-H$  group through the ring). Selected distances are shown in Å.

internally stabilize the carbocations. Shown in Figures 3c–d are  $NH_2^+$  and  $CH_2$  congeners, again transition state structures; for these systems the  $C_5-C_6-C_7$  bond angle likely increases due to transannular steric clashes.

To further examine, and separate, the impact of having a charge and a formally empty p-orbital at  $C_{10}$  on the transannular  $C-H\cdots C^+$  interactions that “lock” the  $C_{sp^2}-H$  bond with the  $C^+$  (e.g., Figure 3a), IRCs corresponding to the  $C_6,C_7$ -prenyl flip were calculated for the  $BH$  and  $NH_2^+$  congeners (Figure 4). In each case, as the prenyl group sweeps from one orientation to the other, there is no geometric evidence that the  $C_{sp^2}-H$  interacts favorably with the empty p-orbital on the boron (Figure 4, top) or the positive charge of the  $NH_2^+$  group (Figure 4, bottom). In both cases, as the prenyl group rotates through the ring there is a corresponding increase in energy from various sources of strain. In the  $B_{10}$  case, if there were a  $C_{sp^2}-H\cdots(p\text{-orbital})$  transannular interaction, it likely would be revealed by a deviation from the smooth curve that is observed as the  $C_{sp^2}-H$  explores the interior of the macrocycle (Figure 4, top). Likewise, there is no change to the smooth curve as the  $C_{sp^2}-H$  sweeps past the  $NH_2^+$  group, again indicating no favorable interaction (Figure 4, bottom). The corresponding geometry (as defined by the  $C_7-C_6-H_6-C_{10}$  dihedral angle) of the  $C_{sp^2}-H\cdots C^+$  transannular interaction (a minimum on its potential energy surface; Figure 3a) is highlighted in each case by the red dot on the IRC curve. Two other  $C_{10}$ -carbocation systems featuring the transannular  $C-H\cdots C^+$  interactions and their  $BH$  and  $NH_2^+$  congeners were examined and similar results were obtained (see Supporting Information; control experiments with  $CH_2$  congeners were performed as well). These experiments demonstrate clearly that both the positive charge and the empty p-orbital are required for favorable  $C_{sp^2}-H\cdots C^+$  transannular interaction.

**4. Interplay of Stabilizing Features.** In this section we describe examples of scenarios where several of the stabilizing factors described above come into play in controlling reactivity.

A transition state structure was located for a conformational change of the humulyl cation whose imaginary frequency was associated with a motion that mainly involves the  $CH^+$  group wagging in and out of the ring (Figure 5). As the  $CH^+$  group folds into the ring (Figure 5, right), it interacts with the  $C_2=C_3$   $\pi$ -bond, leading to a structure whose carbocation center is strongly pyramidalized (sum of the three  $C-C-C/H$  angles =  $341^\circ$ ). In fact, this interaction has been taken to the extent of significant covalency, with a  $C_{10}-C_2$  distance (1.72 Å) that is not unusual for a strongly hyperconjugated  $C-C$  bond.<sup>2,13</sup> Consequently, this structure is better viewed as a caryophyllyl cation, a direct precursor to caryophyllene (Scheme 1).<sup>2</sup>

In contrast, as the  $CH^+$  group folds out of the ring (Figure 5, left), it partakes of strong hyperconjugation, similar to that observed for the humulyl cation conformer shown in Figure 1a. This reaction, which has a low barrier (approximately 2 kcal mol<sup>-1</sup> in the ring-closing direction), highlights the flexibility of the humulyl cation; rotations around many of its  $C-C$  bonds are facile, and at every twist and turn there is some means of sating the electron deficiency of its carbocation center. Two related structures in which the 4-membered ring is fully formed are shown in Figure 6, one with *trans* hydrogens at the ring fusion and the other with *cis* hydrogens.<sup>2</sup> In these structures, the newly formed carbocation center at  $C_3$  interacts with the remaining  $C_6=C_7$   $\pi$ -bond with  $C_3^+---C_6$  distances as short as 2.07 Å. In addition,  $C-C$  and  $C-H$  bonds oriented (nearly) coplanar to the empty p-orbital on  $C_3$  exhibit evidence of hyperconjugation. Overall, even after the new  $C_{10}-C_2$  bond is formed, similar stabilizing features are observed.

In the boron-substituted version of the conformational change, as the corresponding  $B_{10}-H$  bond wags toward the



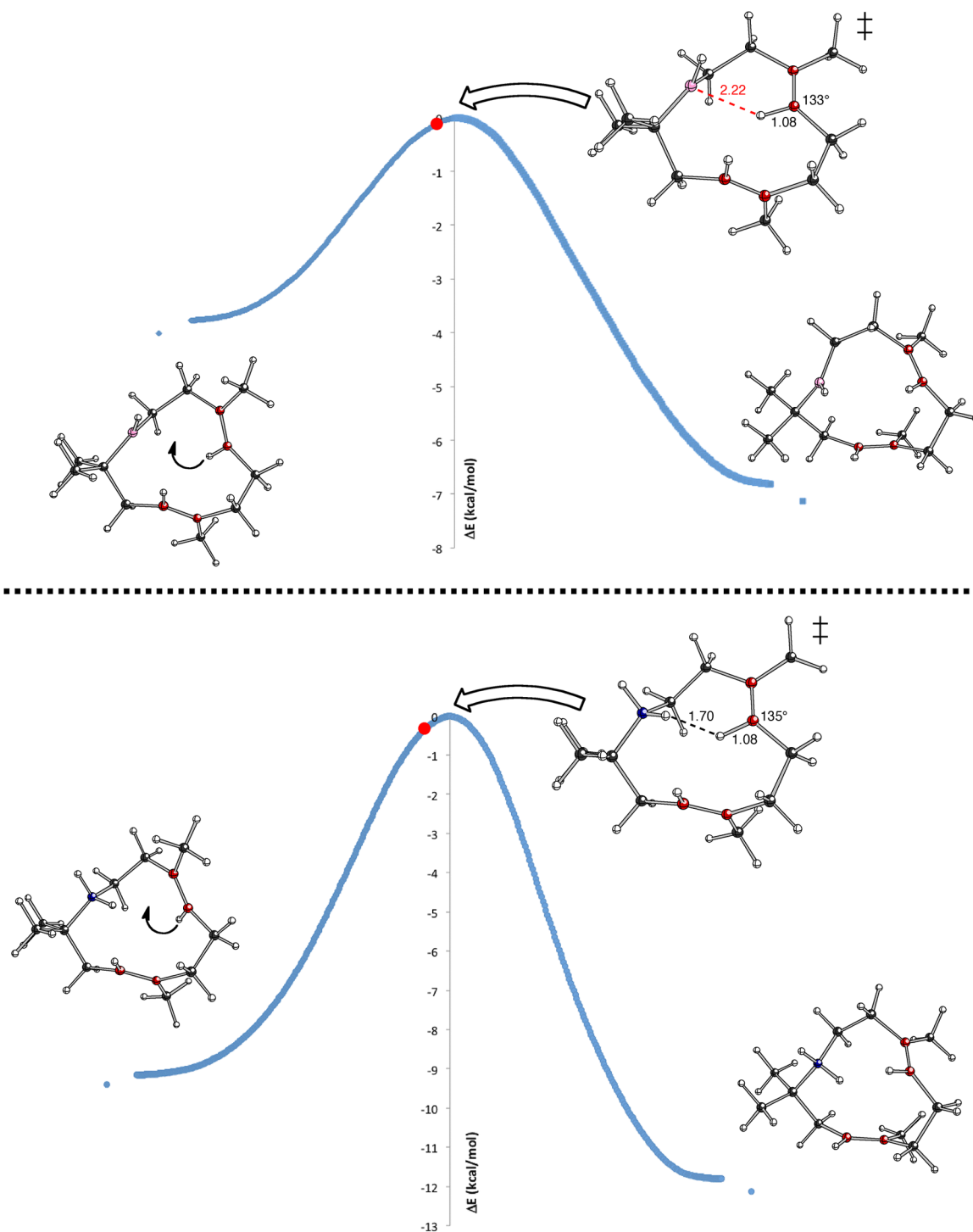


**Figure 4.** Rotation of the  $C_6,C_7$ -prenyl group in a  $B_{10}$  congener (top) and  $N_{10}$  congener (bottom) of the humulyl cation. Energies are relative to the energy of the transition state structure in each case. The red dots correspond to the  $C_7-C_6-H_6-X_{10}$  dihedral angle identical to that found in the humulyl cation minimum (Figure 3a). The isolated points at the ends of the IRCs are the results of optimization from the final points of the IRCs, offset from the curves by an arbitrary distance.

$C_2=C_3$   $\pi$ -bond, it does not form a C–B bond (see Supporting Information for IRC). When the  $B_{10}$ –H bond wags away from the center of the ring, it does not stop (unlike the humulyl cation; Figure 5). Rather, the borane group rotates beyond the equator of the ring, until it picks up electron density from the other side of the ring. In contrast, the  $NH_2^+$  system shows a clear energetic preference (12–14 kcal/mol) for the positively charged group to be oriented toward the center of the ring as

one  $N-H^{\delta+}$  orients itself toward the  $\pi$ -bonds. Although a new bond cannot be made, as in the caryophyllyl cation in Figure 5, an interaction between the positively charged group and  $\pi$ -electron density does lead to a similar conformational preference (see Supporting Information for IRC).

Another caryophyllyl structure can be generated by protonation of  $\beta$ -koraie (Scheme 2).  $\beta$ -Koraie is a tricyclic sesquiterpene related to the natural product koraol,<sup>20</sup> itself

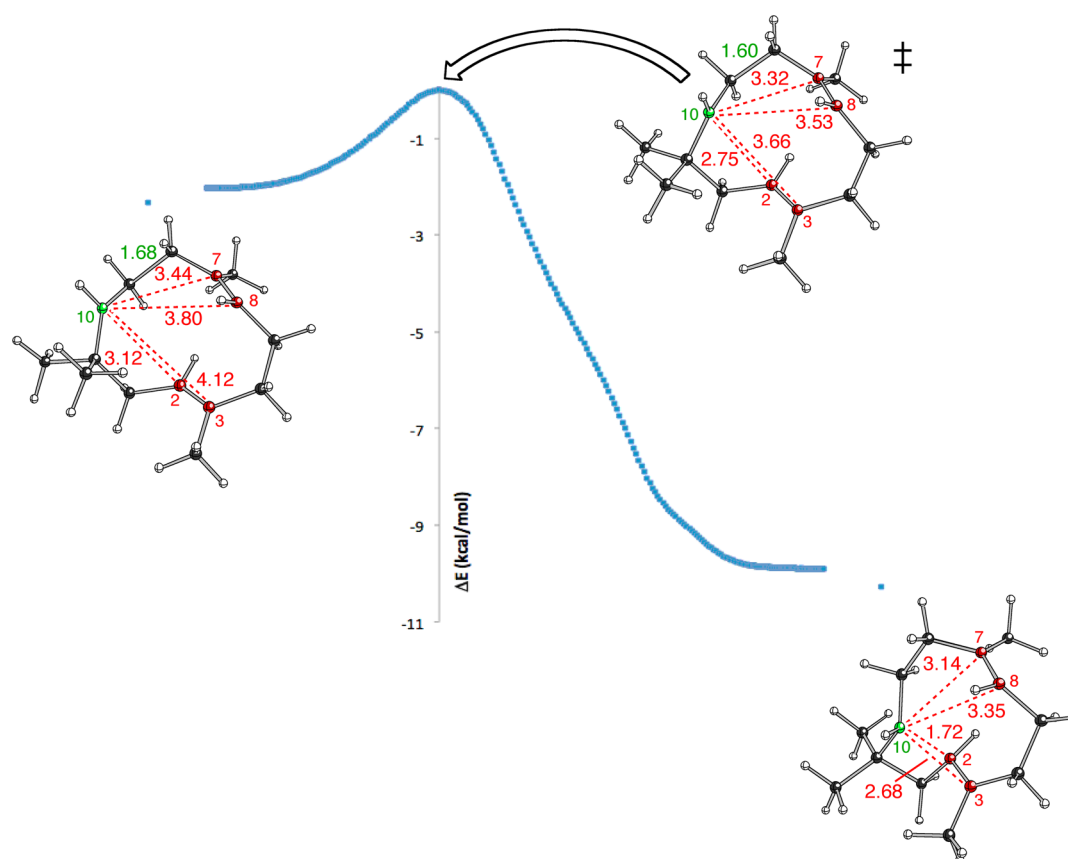


Figure 5. IRC plot for interconversion of two conformers of the humulyl cation. Selected distances are shown in Å.

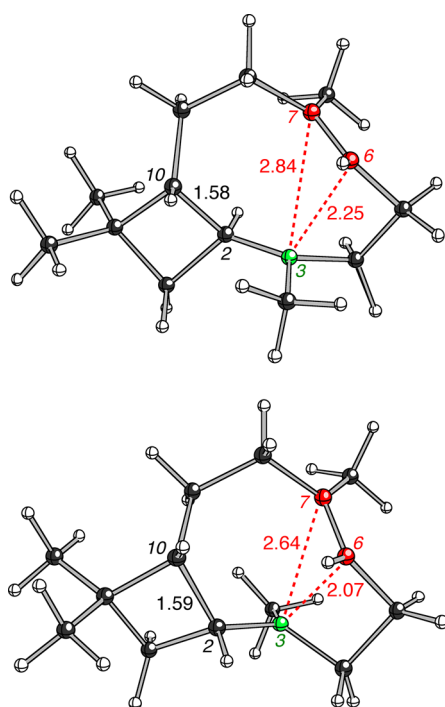
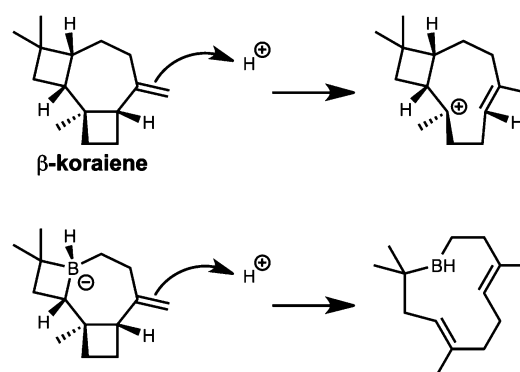


Figure 6. Two structures resembling the caryophyllyl cation (with *trans* and *cis* hydrogens at the ring fusion). Selected distances are shown in Å.

likely biosynthesized from the humulyl cation via a caryophyllyl cation intermediate.<sup>21</sup> Protonation of  $\beta$ -koraïene at the exocyclic methylene ( $C_7=CH_2$ ) results in the caryophyllyl

#### Scheme 2



cation structure shown at the bottom of Figure 6. However, the  $B_{10}$  congener of koraïene unzips all the way to a monocyclic humulyl cation-like structure (Scheme 2). This result is consistent with the IRC data for the  $B_{10}$ -H wag (Supporting Information) that indicate there is no considerable interaction between  $X_{10}$  and  $C_2$  when the p-orbital is present but the positive charge is absent.

## CONCLUSIONS

The humulyl cation provides a framework that can support several flavors of carbocation delocalization: hyperconjugation, transannular  $\pi(\text{alkene})\cdots C^+$  and transannular  $C-H\cdots C^+$  interactions. Each of these interactions provides an avenue for delocalizing electron density and positive charge. Which interactions predominate for a given conformation appears to result from the proximity of the (potentially) interacting

groups. We have found no conformations of the humulyl cation that do not exploit at least one of these delocalization modes.<sup>22</sup> Substitution of the CH<sup>+</sup> center by BH, NH<sub>2</sub><sup>+</sup>, or CH<sub>2</sub> groups decreases delocalization, often to the point of nothingness, highlighting the impetus for delocalization associated with carbenium substructures that pushes these centers toward the realm of carbonium ions.<sup>14</sup> The structural phenomena observed and discussed in this paper have multiple counterparts found in several structurally contiguous humulyl frameworks (see Supporting Information). These parallel data sets demonstrate that the effects of the substitutions in Table 1 have a consistent impact, independent of the overall conformation of the macrocycle. Our studies also suggest that caution is in order when interpreting atomic substitution data, particularly when distinguishing electronic versus coulombic interactions, as structures containing boron do not simply act as carbenium ions lacking charge.<sup>23</sup>

## ■ ASSOCIATED CONTENT

### ■ Supporting Information

Coordinates and energies for all computed structures and additional IRC data. This material is available free of charge via the Internet at <http://pubs.acs.org>.

## ■ AUTHOR INFORMATION

### Corresponding Authors

\*E-mail: [chamann@albright.edu](mailto:chamann@albright.edu).

\*E-mail: [djtantillo@ucdavis.edu](mailto:djtantillo@ucdavis.edu).

### Present Address

†Trevor A. Hamlin, Department of Chemistry, University of Connecticut, 55 North Eagleville Rd., Storrs, Connecticut 06269-3060, United States.

### Notes

The authors declare no competing financial interest.

## ■ ACKNOWLEDGMENTS

We gratefully acknowledge support from the National Science Foundation (CHE-0957416, CHE030089 for supercomputing resources), and the Undergraduate Research Committee and the Professional Council at Albright College.

## ■ REFERENCES

- (1) (a) Christianson, D. W. *Chem. Rev.* **2006**, *106*, 3412–3442. (b) Christianson, D. W. *Curr. Opin. Chem. Biol.* **2008**, *12*, 141–150. (c) Croteau, R. *Chem. Rev.* **1987**, *87*, 929–954. (d) Cane, D. E. *Sesquiterpene biosynthesis: cyclization mechanisms*; Elsevier: London, 1999; Vol. 2, pp 155–200. (e) Cane, D. E. *Acc. Chem. Res.* **1985**, *18*, 220–226. (f) Cane, D. E. *Chem. Rev.* **1990**, *90*, 1089–1103. (g) Davis, E. M.; Croteau, R. *Top. Curr. Chem.* **2000**, *209*, 53–95.
- (2) (a) Tantillo, D. J. *Chem. Soc. Rev.* **2010**, *39*, 2847–2854. (b) Gutta, P.; Tantillo, D. J. *J. Am. Chem. Soc.* **2006**, *128*, 6172–6179. (c) Hong, Y. J.; Irmisch, S.; Wang, S. C.; Garms, S.; Gershenzon, J.; Zu, L.; Kollber, T. G.; Tantillo, D. J. *Chem.—Eur. J.* **2013**, *19*, 13590–13600. (d) Wang, S. C.; Tantillo, D. J. *Org. Lett.* **2008**, *10*, 4827–4830. (e) Nguyen, Q. N. N.; Tantillo, D. J. *Bestein J. Org. Chem.* **2013**, *9*, 323–331. (f) Hong, Y. J.; Tantillo, D. J. *Chem. Soc. Rev.* **2014**, *43*, 5042–5050.
- (3) (a) Tantillo, D. J. *Nat. Prod. Rep.* **2011**, *28*, 1035–1053. (b) Tantillo, D. J. *Nat. Prod. Rep.* **2013**, *30*, 1079–1086.
- (4) (a) This is part 14 of our series on theoretical studies of sesquiterpene forming carbocation rearrangements. For part 13, see: Pemberton, R. P.; Ho, K. C.; Tantillo, D. J. *Chem. Sci.* **2015**, *6*, 2347–2353. (b) For preliminary theoretical work on altering the structure and reactivity of carbocations through interactions with active site residues, see ref 12a.
- (5) (a) GAUSSIAN03, revision D.01: Frisch, M. J.; Trucks, G. W.; Schlegel, H. B.; Scuseria, G. E.; Robb, M. A.; Cheeseman, J. R.; Montgomery, J. A., Jr.; Vreven, T.; Kudin, K. N.; Burant, J. C.; Millam, J. M.; Iyengar, S. S.; Tomasi, J.; Barone, V.; Mennucci, B.; Cossi, M.; Scalmani, G.; Rega, N.; Petersson, G. A.; Nakatsuji, H.; Hada, M.; Ehara, M.; Toyota, K.; Fukuda, R.; Hasegawa, J.; Ishida, M.; Nakajima, T.; Honda, Y.; Kitao, O.; Nakai, H.; Klene, M.; Li, X.; Knox, J. E.; Hratchian, H. P.; Cross, J. B.; Bakken, V.; Adamo, C.; Jaramillo, J.; Gomperts, R.; Stratmann, R. E.; Yazyev, O.; Austin, A. J.; Cammi, R.; Pomelli, C.; Ochterski, J. W.; Ayala, P. Y.; Morokuma, K.; Voth, G. A.; Salvador, P.; Dannenberg, J. J.; Zakrzewski, V. G.; Dapprich, S.; Daniels, A. D.; Strain, M. C.; Farkas, O.; Malick, D. K.; Rabuck, A. D.; Raghavachari, K.; Foresman, J. B.; Ortiz, J. V.; Cui, Q.; Baboul, A. G.; Clifford, S.; Cioslowski, J.; Stefanov, B. B.; Liu, G.; Liashenko, A.; Piskorz, P.; Komaromi, I.; Martin, R. L.; Fox, D. J.; Keith, T.; M. A. Al-Laham, Peng, C. Y.; Nanayakkara, A.; Challacombe, M.; Gill, P. M. W.; Johnson, B.; Chen, W.; Wong, M. W.; Gonzalez, C.; Pople, J. A.; Gaussian, Inc., Wallingford, CT, 2004. (b) *Gaussian 09*, revision B.01: Frisch, M. J.; Trucks, G. W.; Schlegel, H. B.; Scuseria, G. E.; Robb, M. A.; Cheeseman, J. R.; Scalmani, G.; Barone, V.; Mennucci, B.; Petersson, G. A.; Nakatsuji, H.; Caricato, M.; Li, X.; Hratchian, H. P.; Izmaylov, A. F.; Bloino, J.; Zheng, G.; Sonnenberg, J. L.; Hada, M.; Ehara, M.; Toyota, K.; Fukuda, R.; Hasegawa, J.; Ishida, M.; Nakajima, T.; Honda, Y.; Kitao, O.; Nakai, H.; Vreven, T.; Montgomery, J. A., Jr.; Peralta, J. E.; Ogliaro, F.; Bearpark, M.; Heyd, J. J.; Brothers, E.; Kudin, K. N.; Staroverov, V. N.; Keith, T.; Kobayashi, R.; Normand, J.; Raghavachari, K.; Rendell, A.; Burant, J. C.; Iyengar, S. S.; Tomasi, J.; Cossi, M.; Rega, N.; Millam, J. M.; Klene, M.; Knox, J. E.; Cross, J. B.; Bakken, V.; Adamo, C.; Jaramillo, J.; Gomperts, R.; Stratmann, R. E.; Yazyev, O.; Austin, A. J.; Cammi, R.; Pomelli, C.; Ochterski, J. W.; Martin, R. L.; Morokuma, K.; Zakrzewski, V. G.; Voth, G. A.; Salvador, P.; Dannenberg, J. J.; Dapprich, S.; Daniels, A. D.; Farkas, O.; Foresman, J. B.; Ortiz, J. V.; Cioslowski, J.; Fox, D. J., Gaussian, Inc., Wallingford, CT, 2010.
- (6) (a) Becke, A. D. *J. Chem. Phys.* **1993**, *98*, 5648–5652. (b) Becke, A. D. *J. Chem. Phys.* **1993**, *98*, 1372–1377. (c) Lee, C.; Yang, W.; Parr, R. G. *Phys. Rev. B* **1988**, *37*, 785–789. (d) Stephens, P. J.; Devlin, F. J. (e) Chabalowski, C. F.; Frisch, M. J. *J. Phys. Chem.* **1994**, *98*, 11623–11627.
- (7) Grimme, S. J. *Comput. Chem.* **2006**, *27*, 1787–1799.
- (8) (a) Matsuda, S. P. T.; Wilson, W. K.; Xiong, Q. *Org. Biomol. Chem.* **2006**, *4*, 530–543. (b) Schreiner, P. R.; Fokin, A. A.; Pascal, R. A., Jr.; de Meijere, A. *Org. Lett.* **2006**, *8*, 3635–3638. (c) Wodrich, M. D.; Corminboeuf, C.; Schleyer, P. v. R. *Org. Lett.* **2006**, *8*, 3631–3634.
- (9) (a) Fukui, K. *Acc. Chem. Res.* **1981**, *14*, 363–368. (b) Gonzalez, C.; Schlegel, H. B. *J. Chem. Phys.* **1989**, *90*, 2154–2161. (c) Gonzalez, C.; Schlegel, H. B. *J. Chem. Phys.* **1991**, *95*, 5853–5860. (d) Maeda, S.; Harabuchi, Y.; Ono, Y.; Taketsuga, T.; Morokuma, K. *Int. J. Quantum Chem.* **2015**, *115*, 258–269.
- (10) Müller, N.; Falk, A.; Gsaller, G. *Ball & Stick V.4.0a12, molecular graphics application for MacOS computers*; Johannes Kepler University: Linz, 2004.
- (11) (a) Miklis, P. C.; Ditchfield, R.; Spencer, T. A. *J. Am. Chem. Soc.* **1998**, *120*, 10482–10489. (b) Dougherty, D. A. *Science* **1996**, *271*, 163–168. (c) Faraldos, J. A.; Antonczak, A. K.; Gonzalez, V.; Fullerton, R.; Tippmann, E. M.; Allemann, R. K. *J. Am. Chem. Soc.* **2011**, *133*, 13906–13909. (d) Jenson, C.; Jorgensen, W. L. *J. Am. Chem. Soc.* **1997**, *119*, 10846–10854.
- (12) (a) Hong, Y. J.; Tantillo, D. J. *Chem. Sci.* **2013**, *4*, 2512–2518. (b) Nishio, M. *Phys. Chem. Chem. Phys.* **2011**, *13*, 13873–13900. (c) Takahashi, O.; Kohno, Y.; Nishio, M. *Chem. Rev.* **2010**, *110*, 6049–6076. (d) Steiner, T. *Angew. Chem., Int. Ed.* **2002**, *41*, 48–76.
- (13) (a) For a recent review of hyperconjugation as evaluated using computational techniques, see: Alabugin, I. V.; Gilmore, K. M.; Peterson, P. W. *WIREs Comput. Mol. Sci.* **2011**, *1*, 109–141. (b) For a review focused on hyperconjugation in carbocations, see: Wu, J. I.; Schleyer, P. v. R. *Pure Appl. Chem.* **2013**, *85*, 921–940.

(14) (a) Brown, H. C. (with comments by P. v. R. Schleyer), *The Nonclassical Ion Problem*; Plenum: New York, 1977. (b) Issue 12 of *Acc. Chem. Res.* 1983, 16.

(15) (a) Due to the geometric constraints of the 11-membered macrocycle, it is difficult to compare this to other van der Waals complexes with more degrees of freedom. (b) Zhao, X.; Stephan, D. W. *J. Am. Chem. Soc.* **2011**, 133, 12448–12450. (c) Mantina, M.; Chamberlin, A. C.; Valero, R.; Cramer, C. J.; Truhlar, D. G. *J. Phys. Chem. A* **2009**, 113, 5806–5812.

(16) Tantillo, D. J. *J. Phys. Org. Chem.* **2008**, 21, 561–570.

(17) Leading references on alkenyl carbocations: (a) Rappoport, Z.; Apeloig, Y. *J. Am. Chem. Soc.* **1974**, 96, 6428–6436. (b) Hanack, M. *Acc. Chem. Res.* **1976**, 9, 364–371. (c) Okuyama, T. *Acc. Chem. Res.* **2002**, 35, 12–18. (d) Müller, T.; Juhasz, M.; Reed, C. A. *Angew. Chem., Int. Ed.* **2004**, 116, 1569–1572.

(18) (a) Kirchen, R. P.; Sorensen, T. S. *J. Chem. Soc., Chem. Commun.* **1978**, 769–770. (b) Sorensen, T. S.; Whitworth, S. M. *J. Am. Chem. Soc.* **1990**, 112, 8135–8144. (c) McMurry, J. E.; Hodge, C. N. *J. Am. Chem. Soc.* **1984**, 106, 6450–6451. (d) McMurry, J. E.; Lectka, T.; Hodge, C. N. *J. Am. Chem. Soc.* **1989**, 111, 8867–8872. (e) Ponec, R.; Yuzhakov, G.; Tantillo, D. J. *J. Org. Chem.* **2004**, 69, 2992–2996. (f) See the Supporting Information for a picture of a typical delocalized orbital showing a 3-center C··H··C<sup>+</sup> interaction.

(19) Hong, Y. J.; Tantillo, D. J. *Chem. Sci.* **2010**, 1, 609–614.

(20) Khan, V. A.; Gatilov, Y. V.; Dubovenko, Z. V.; Pentegova, V. A. *Khim. Prir. Soedin.* **1979**, 15, 652; *Chem. Nat. Compd. (Engl. Transl.)* **1979**, 15, 572–576.

(21) Isegawa, M.; Maeda, S.; Tantillo, D. J.; Morokuma, K. *Chem. Sci.* **2014**, 5, 1555–1560.

(22) The presence of these interactions in conformation-exchanging transition state structures will be discussed in a subsequent report on humulyl cation conformational interconversions.

(23) Leading references on boron-for-carbon substitutions in various contexts: (a) Kürti, L.; Chein, R.-J.; Corey, E. J. *J. Am. Chem. Soc.* **2008**, 130, 9031–9036. (b) Li, G.; Xiong, W.-W.; Gu, P.-Y.; Cao, J.; Zhu, J.; Ganguly, R.; Li, Y.; Grimsdale, A. C.; Zheng, Q. *Org. Lett.* **2015**, 17, 560–563. (c) Firouzi, R.; Sharifi Ardani, S. *Phys. Chem. Chem. Phys.* **2014**, 16, 11538–11548. (d) Piers, W. E.; Bourke, S. C.; Conroy, K. D. *Angew. Chem., Int. Ed.* **2005**, 44, 5017–5036.